energies

MDPI

Article

A Numerical Study on the Performance Evaluation of a Semi-Type Floating Offshore Wind Turbine System According to the Direction of the Incoming Waves

Hyeonjeong Ahn, Yoon-Jin Ha, Su-gil Cho, Chang-Hyuck Lim and Kyong-Hwan Kim *

Korean Research Institute of Ship & Ocean Engineering, Daejeon 34103, Korea; ahnh@kriso.re.kr (H.A.); yj_ha0811@kriso.re.kr (Y.-J.H.); sgcho@kriso.re.kr (S.-g.C.); ckdgur1092@kriso.re.kr (C.-H.L.)
* Correspondence: kkim@kriso.re.kr; Tel.: +82-42-866-3941

Abstract: In this study, the performance evaluation of a semi-type floating offshore wind turbine system according to the direction of the incoming waves is investigated. The target model in this this study is a DTU 10 MW reference wind turbine and a LIFES50+ OO-Star Wind Floater Semi 10 MW, which is the semisubmersible platform. Numerical simulation is performed using FAST developed by National Renewable Energy Laboratory (NREL), which is an aero-hydro-servo-elastic fully coupled simulation tool. The analysis condition used in this study is the misalignment condition, which is the wind direction fixed at 0 degree and the wave direction changed at 15 degrees intervals. In this study, two main contents could be confirmed. First, it is confirmed that sway, roll, and yaw motions occur even though the direction of the incoming waves is 0 degree. The cause of the platform's motion such as sway, roll and yaw is the turbulent wind and gyroscope phenomenon. In addition, the optimal value for the nacelle–yaw angle that maximizes the rotor power and minimizes the tower load is confirmed by solving the multiobjective optimization problem. These results show the conclusion that setting the initial nacelle–yaw angle can reduce the tower load and get a higher generator power. Second, it is confirmed that the platform's motion and loads may be underestimated depending on the interval angle of incidence of the wind and waves. In particular, through the load diagram results, it is confirmed that most of the results are asymmetric, and the blade and tower loads are especially spiky. Through these results, the importance of examining the interval angle of incidence of the wind and waves is confirmed. Unlike previous studies, this will be a more considerable issue as turbines become larger and platforms become more complex.

Keywords: floating offshore wind turbine system; semisubmersible; asymmetric thrust; directionality; misalignment

Citation: Ahn, H.; Ha, Y.-J.; Cho, S.-g.; Lim, C.-H.; Kim, K.-H. A Numerical Study on the Performance Evaluation of a Semi-Type Floating Offshore Wind Turbine System According to the Direction of the Incoming Waves. *Energies* **2022**, *15*, 5485. https://doi.org/10.3390/en15155485

Academic Editor: Hua Li

Received: 5 July 2022
Accepted: 26 July 2022
Published: 28 July 2022

1. Introduction

In the case of a fixed offshore wind turbine system, since most of the supporting structures are axisymmetric, the direction of the incoming environmental load does not significantly affect the overall structural loads. Therefore, it is mainly assumed that the wind, waves and currents come from the same direction, but this may be somewhat conservative depending on the location where the wind turbine is installed and the shape of the platform. Among the platforms of floating offshore wind turbine system, especially in the case of the semisubmersible type consisting of several columns, since it is not axisymmetric, the direction of the incoming wind, waves and currents can have a greater effect on the structural load in the platform's motion compared to the cylindrical spar platform.

In IEC61400-3-2, the international design standard for floating offshore wind turbine systems, it is proposed to calculate the load according to the direction of the incoming wind and waves to find the extreme load acting on the total system. Since the directions of the incoming wind, waves and currents in real sea conditions are not always the

same, it is necessary to find the direction of the incoming wind and waves at which the extreme loads appear. If there are no data on real sea conditions, a load analysis should be performed by dividing the interval angle of incidence of the wind and waves by 30 degrees. In this regard, various studies have been conducted on the performance evaluation of floating offshore wind turbine systems according to the direction of the incoming marine environmental loads. Bachynski et al. [1] performed a fatigue load evaluation of the tower base according to the direction of the incoming wind and waves for a floating offshore wind turbine system to which spar [2], semisubmersible [3], and TLP platforms were applied. It was confirmed that the fatigue load at the tower base occurred the most in the codirectional condition. Barj et al. [4] performed a numerical simulation for the performance evaluation on a spar platform by changing the direction of the incoming waves at 15 degrees intervals. It was shown that it was possible to predict the maximum value of the load of the system even using the interval angle of incidence of the wind and waves of 30 degrees. In addition, they observed the importance of the 90 degrees and −90 degrees wind/wave misalignment for the side-to-side wind turbine loadings; the fairlead and anchor loads for three mooring lines experienced more significant loads in waves directed along the mooring line. Stewart et al. [5] calculated the ultimate load and fatigue load occurring in the blade root part, tower, and mooring system of the spar and semisubmersible platforms. Since the interval angle of incidence of the wind and waves recommended by the IEC61400-3-2 [6], which is the international design standard for floating offshore wind turbine system, is rather conservative and requires a high computational power, it has been suggested to apply only 0 degree and 90 degrees for the efficiency of load calculations. Oh et al. [7] performed a model test and numerical simulation according to the direction of the incoming wind on the semisubmersible platform, and the load of the tower base was greatest when the directions of the incoming wind and waves were the same. However, it was confirmed that that standard deviation was similar to the condition when the directions of the incoming wind and waves were different. Lyu et al. [8] performed a numerical simulation to find the roles of the wind and wave directions using the NREL 5 MW reference wind turbine [9] and spar platform. As a results, the longitudinal modes of the system such as surge and pitch motion primarily relied on wind loads, while the transverse modes of the system such as sway and roll primarily relied on wave loads. In particular, the yaw motion was shown to be of maximum value when the wave direction was 90 degrees, but the value was only 3 degrees. Li et al. [10] performed a numerical simulation under regular waves to explore the effects of the yaw error and the wind–wave misalignment on the dynamic characteristics of the floating offshore wind turbine system using the NREL 5 MW reference wind turbine semisubmersible platform. As a results, they confirmed that the yaw error and the wind–wave misalignment were closely related to the performances of the FOWT, so the influence of the yaw error and the wind–wave misalignment must be considered together. Özina et al. [11] performed a numerical simulation under various environmental conditions to evaluate the platform's motion and damage equivalent loads of the mooring line tensions of the OO-Star Wind Floater Semi 10 MW. The results indicated that a wind–wave misalignment led to a complex coupled response of the floating offshore wind turbines at slightly above-rated wind speed.

This paper introduces the importance of an evaluation platform of the yaw motion in large floating offshore wind turbine system as well as the need for the subdivision of the interval angle of incidence of the wind and waves for asymmetric and spiky loads acting on the platform, blade and tower. In order to provide the results of the previously mentioned aims, the performance evaluation of a semi-type floating offshore wind turbine system according to the direction of the incoming waves is investigated. The target model in this study is a DTU 10 MW reference wind turbine and a LIFES50+ OO-Star Wind Floater Semi 10 MW which is a semisubmersible platform. The analysis condition used in this study is the misalignment condition, which means the wind direction is fixed at 0 degree and the wave direction is changed at 15 degrees intervals.

Previously, the model used in the most similar study was a 5 MW reference wind turbine and a simple cylindrical platform called an OC3 spar-type. Therefore, the asymmetry of the platform's motion and loads were not evident. In this study, the platform's motion and loads asymmetry in wind turbines with the interval angle of incidence of the wind and waves are presented and analyzed. The reason why this study is necessary is that as wind turbines become larger and platforms become more complex, there may be a large difference in platform's motion and loads depending on the interval angle of incidence of the wind and waves. These results can be presented as a sufficient basis for the establishment of an international design standard for floating offshore wind turbine systems.

The remainder of this paper is organized as follows: Section 2 details the target model and validation of the numerical setup. Section 3 describes the results of the platform's motion and loads according to the direction of the incoming waves and the interval angle of incidence of wind and waves. Conclusions are found in Section 4.

2. Numerical Setup

2.1. Target Model

In this study, the numerical simulation of the floating offshore wind turbine system was performed using FAST v8 [12], which is a representative analysis tool for wind turbine system. FAST joins aerodynamics models, hydrodynamics models for offshore structures, control and electrical system (servo) dynamics models and structural (elastic) dynamics models to enable a coupled nonlinear aero-hydro-servo-elastic simulation in the time domain. In order to evaluate the performance of the floating offshore wind turbine system according to the direction of the incoming wind and waves, the DTU 10 MW reference wind turbine [13] and the OO-Star Wind Floater Semi 10 MW platform [14,15] proposed by LIFES50+ project were used. Figure 1 shows the OO-Star Wind Floater Semi 10 MW, and Tables 1–3 summarize the main specifications of the DTU 10 MW reference wind turbine and OO-Star Wind Floater Semi 10 MW.

Figure 1. LIFES50+ OO-Star Wind Floater Semi 10 MW.

Table 1. Overall parameters of the DTU 10 MW reference wind turbine.

Parameter	Unit	Value
Rotor orientation	(-)	Clockwise, upwind
Rated power	(MW)	10.0
Rotor diameter	(m)	178.3
Hub height	(m)	119.0
Cut-in, rated, cut-out wind speed	(m/s)	4.0, 11.4, 25.0
Minimum, maximum rotor speed	(rpm)	6.0, 9.6
Rotor mass	(kg)	228,000
Nacelle mass	(kg)	446,000

Table 2. Overall parameters of the LIFES50+ OO-Star Wind Floater Semi.

Parameter	Unit	Value
Overall substructure mass (excl. tower, mooring)	(kg)	21,709,000
Centre of mass (CM) below MSL	(m)	15.255
Substructure roll inertia about CM	(kgm^2)	9,430,000,000
Substructure pitch inertia about CM	(kgm^2)	9,430,000,000
Substructure yaw inertia about CM	(kgm^2)	16,300,000,000
Tower base interface above MSL	(m)	11.0
Draft at equilibrium position with mooring (no thrust)	(m)	22.0
Displaced water volume	(m^3)	23,509
Centre of buoyancy below MSL	(m)	14.236

Table 3. Overall parameters of the LIFES50+ OO-Star Wind Floater Semi mooring system.

Parameter	Unit	Value
Number of lines	(-)	3
Angle between adjacent lines	(deg.)	120
Vertical position of fairleads above MSL	(m)	9.5
Radius to anchors from platform centerline	(m)	691
Radius to fairleads from platform centerline	(m)	44
Pretension	(N)	1,670,000

2.2. Validation of the FAST Numerical Model

To verify the setup of the FAST numerical model, some responses under the same conditions as LIFES50+ D4.5 were compared. Figure 2 shows the response to irregular waves and turbulent wind in extreme conditions. Turbulent wind generally refers to rapid fluctuations in wind velocity. The design load case was 6.1 with V = 44 m/s, HS = 10.9 m and TP = 16.0 s, therefore the turbine was parked, with the blades in feather position. These load cases were run for 5400 s to be able to remove 1800 s of transient, and Figure 2 shows only a part of the time series results.

2.3. Environmental Conditions

In this study, the marine environmental conditions in the East Sea were considered for DLC1.2, which is the operational condition, among the design load cases proposed in IEC61400-3-2. The wind speed used for the performance evaluation was 11.4 m/s, which is the rated wind speed of the DTU 10 MW reference wind turbine, and the turbulence intensity "A" was used. "A" is one of the standard IEC categories of turbulence characteristics, with "A" being the most turbulent [16]. The wave used for the performance evaluation was a JONSWAP spectrum with a significant wave height of 2.84 m, a peak period of 7.25 s and peak parameter of 2.5. The current used for the performance evaluation was 0.9 m/s, and this was always the same as the wave direction. In this study, in order to investigate the platform's motion, blade and tower's moments, and the fairlead and anchor tensions of the floating offshore wind turbine system according to the change of the direction of the incoming wind and waves, the nacelle–yaw angle was fixed at 0 degree, and the direction of

the incoming waves was changed. Figure 3 shows the schematic view for the misalignment conditions, which are the main conditions of this study. Figure 3 shows a diagram for the case where the direction of the incoming wind is 0 degree and the direction of the incoming waves are 30, 165 and 315 degrees.

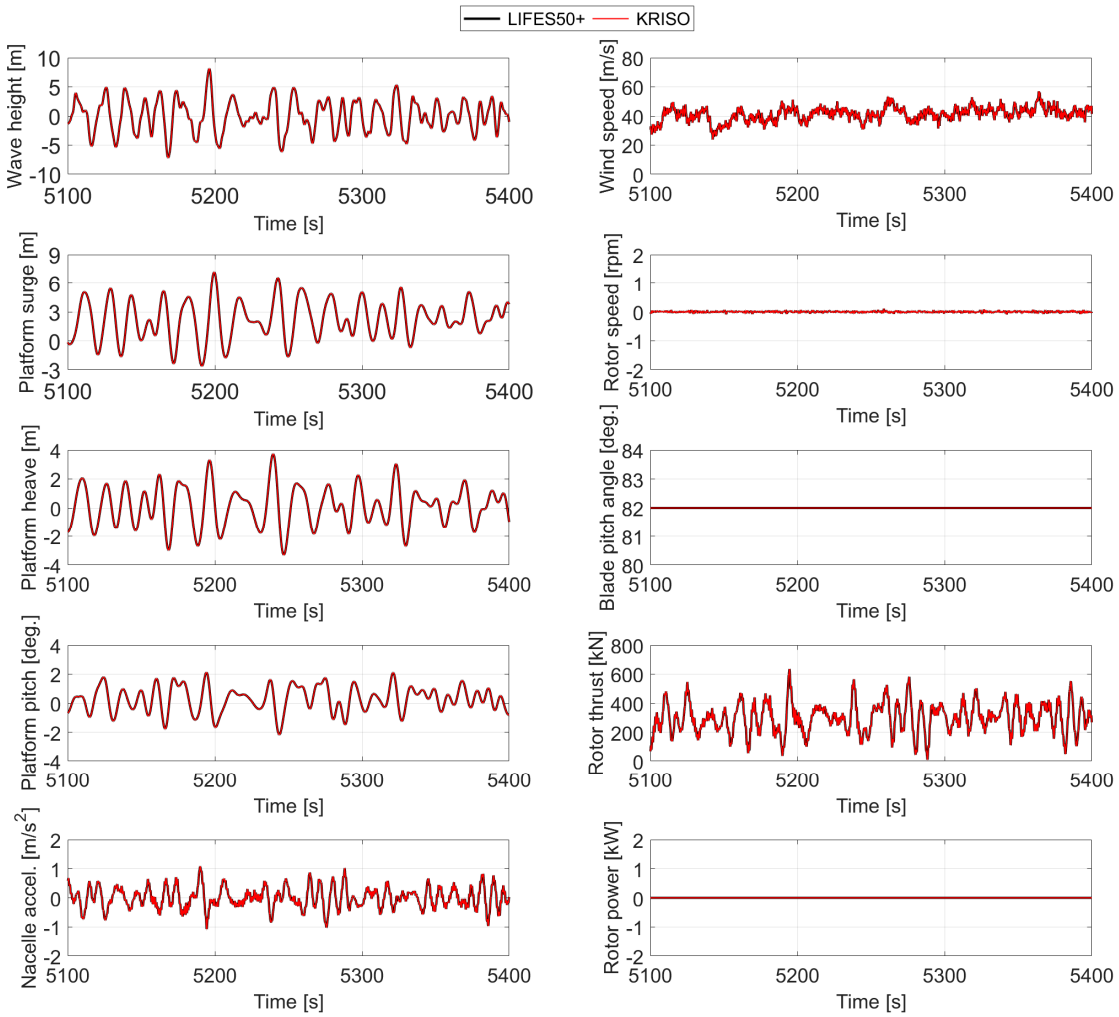

Figure 2. Validation of the responses to DLC6.1 for the OO-Star Wind Floater Semi 10 MW.

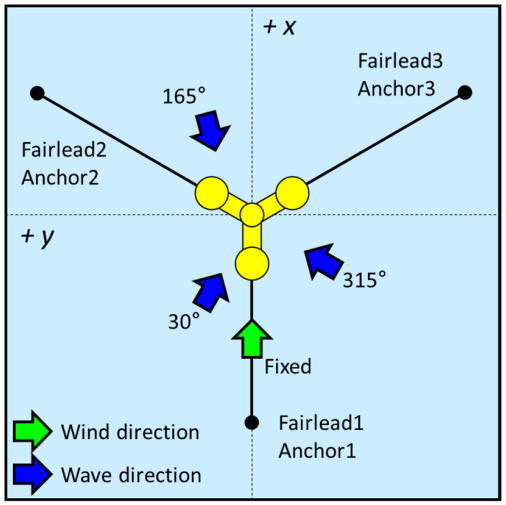

Figure 3. Schematic view for defined wind and waves directions.

3. Results and Discussion

3.1. Platform's Motion and Loads

In this study, the maximum values of the platform's motion, blade and tower's moments, and the fairlead and anchor tensions of the floating offshore wind turbines for 24 wave directions were diagrammed in a load diagram. In order to confirm the characteristics of each direction in detail, the range of values was plotted based on the absolute maximum values in all directions. Figure 4 shows the absolute maximum values of the platforms' motion according to the 24 wave directions. In the case of a surge, sway, heave and pitch, the platform's motion dominant in the direction of the incoming wave can be confirmed. However, in the case of a roll and yaw motion, the maximum values are shown when the directions of the incoming waves are 90 degrees and 210 degrees, respectively. In particular, in the yaw motion, the magnitude of the platform's motion is more than 4 degrees even though the direction of the incoming wave is 0 degree and 180 degrees. This phenomenon is caused by the rotor rotation of the large wind turbine and the turbulent wind, and this is detailed in Section 3.3.

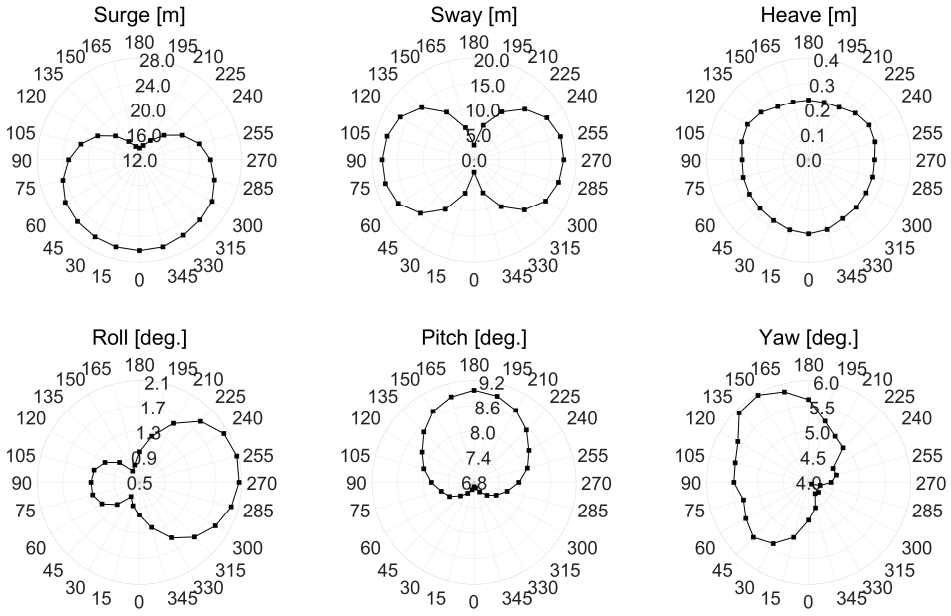

Figure 4. Absolute maximum values of the platform's motion according to the 24 wave directions.

Figure 5 shows the absolute maximum values of the blade and tower's moments according to the 24 wave directions. In Figure 5, the blade and tower's moments show very asymmetrical and spiky results according to the change in the direction of the incoming wind and waves. Barj et al. observed the importance of the 90 degrees and −90 degrees wind/wave misalignment for the side-to-side wind turbine loadings. However, in this study the maximum tower top and tower base moments (x-dir.) occurred at 315 and 300, respectively. Taking these results together, it is necessary to predict the ultimate load and fatigue load with a small interval angle of incidence of the wind and waves. Figure 6 shows the absolute maximum values of the fairlead and anchor tensions according to the 24 wave directions. The fairlead and anchor numbers are shown in Figure 3.

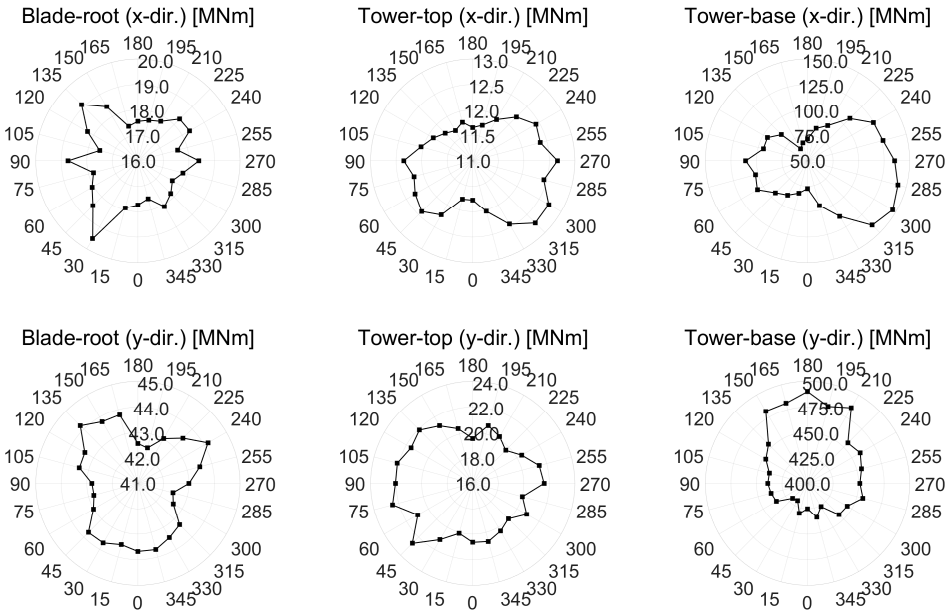

Figure 5. Absolute maximum values of the blade and tower's moments according to the 24 wave directions.

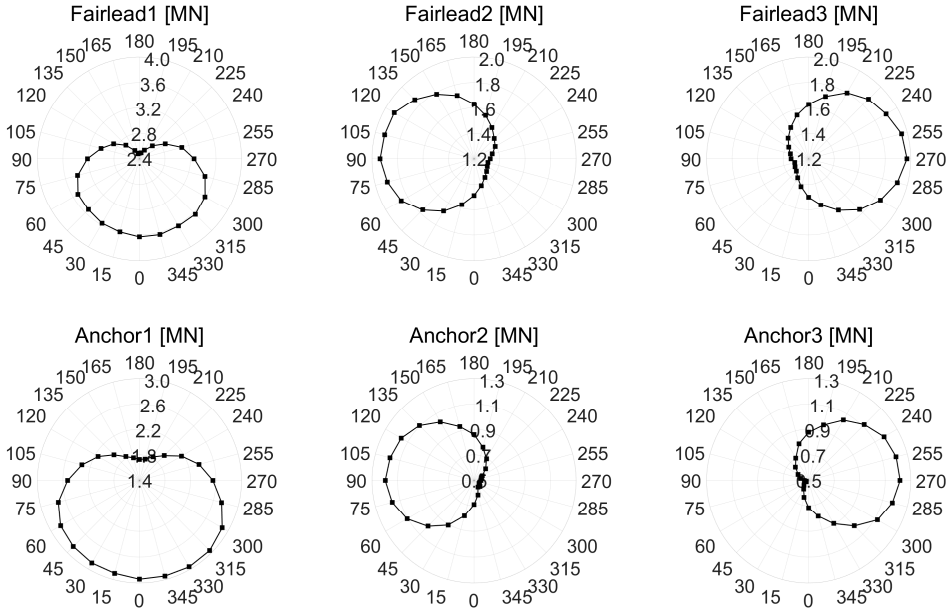

Figure 6. Absolute maximum values of the fairlead and anchor tensions according to the 24 wave directions.

In the Figure 6, the fairlead and anchor tensions had their maximum values near where the mooring lines were placed. Barj et al. observed the fairlead and anchor loads for three mooring lines experienced more significant loads in the waves directed along the mooring line. However, in this study, the maximum fairlead tension occurred at 345, 90 and 270 degrees instead of 0, 120 and 240 degrees. The mooring system was directly connected to the platform, so these results can be seen as a reflection of the asymmetric platform's motion. In other words, the reason the maximum did not occur along the mooring line was due to the influence of the large wind turbine rotating in one direction. Recently, platforms have been enlarged and platforms having various shapes have been developed, and there are often cases where the wind turbine is installed on the side column rather than the center

column of the platform. Therefore, in order to improve the load predictability of a large floating offshore wind turbine system, it seems that the load analysis with a small interval angle of incidence of the wind and waves is needed.

3.2. Platform's Yaw Motion of a Large Floating Offshore Wind Turbines System

3.2.1. Causes of the Platform's Yaw Motion

The transverse motion such as sway, roll and yaw should not occur for the platform with lateral symmetry (symmetric about the xz-plane) in shape and mass distribution. However, as can be seen from the results in Section 3.2, the platform's yaw motion was observed at all wave directions. Therefore, in order to precisely understand the phenomenon of platform's yaw motion, the platform's yaw motion was confirmed under various wind and wave conditions. Table 4 shows the analysis conditions to find the cause of the platform's yaw motion. The wind speed and rotor rotational speed used were rated, and the wave condition was the same as mentioned in Section 2.2. The direction of the wind and waves was the same at 0 degree.

Table 4. Analysis conditions to find the cause of the platform's yaw motion.

Case #	Wind	Wave	Control	
			Rotor Speed	Blade Pitch Angle
Case 1	-	-	9.6 rpm (fixed)	0° (fixed)
Case 2	-	H_S 2.84 m, T_P 7.25 s		
Case 3	11.4 m/s (Steady)	H_S 2.84 m, T_P 7.25 s	9.4~9.8 rpm (Variable)	0~1° (Variable)
Case 4				
Case 5	11.4 m/s (Turbulent)	H_S 2.84 m, T_P 7.25 s		
Case 6				

Figure 7 shows the snapshots when the absolute maximum values of the platform's yaw motion occurred for the six cases mentioned above. The platform's yaw motion hardly appeared in cases 1, 2, 3, and 4, and it was confirmed that it appeared significantly in cases 5 and 6. It can be seen from these snapshots that it was caused by turbulent wind. Not only a yaw motion but also a surge motion of the platform was observed, and it was relatively small under the condition of only the rotor rotation (case 1) or only the wave condition (case 2), but it was observed that the platform's surge motion was large when the wind was applied. As described in Section 3.1, it can be seen that the platform's surge motion was most dominated by the wind.

Figures 8 and 9 show a time series of the platform's yaw motion of some cases defined in Table 4. Figure 8 shows the platform's yaw motion when the wind was steady (case 4) and turbulent (case 6) under the same conditions. In the steady wind condition, although a constant average value appeared for the wind and rotor rotation, the amplitude of the platform's yaw motion hardly appeared. However, in the turbulent wind condition, the amplitude of the platform's yaw motion was relatively large. From this result, it can be seen that the platform's yaw motion was most dominated by the influence of turbulent wind. Figure 9 shows the platform's yaw motion with (case 6) and without (case 5) waves under the same conditions. The platform's yaw motion without waves was larger than the value with waves. From these results, it can be seen that the waves coming from the forward direction was not a dominant external force in the platform's yaw motion.

Figure 10 shows a summary of the results for all analysis conditions defined in Table 4. As can be seen from the results, even in case 1 where there was no external force due to the environmental conditions, the platform's yaw motion occurred only from the rotor rotation. This is because a rotational force is generated as an external force is applied to the rotating rotor. This phenomenon is also called a gyroscope phenomenon [17,18], and it has a higher effect when the moment of inertia or rotational speed of the moving part is large. Therefore, it was not a major consideration for small wind turbines, but it should be

considered in the large wind turbines, in which the rotor radius and RNA mass are greatly increased. In cases 3 and 4, with steady wind, the platform's yaw motion was relatively greater than in cases 1 and 2 without wind. It can be seen that the gyroscope phenomenon was exacerbated due to the wind and waves. However, the platform's yaw motion of case 4 was smaller than that of case 3, which means that the wave reduced the platform's yaw motion as in the result of Figure 10. In cases 5 and 6, it was confirmed that the platform's yaw motion was relatively large due to the gyroscope phenomenon and the aerodynamic instability due to the turbulent wind. This phenomenon may affect the power and tower load combined with the platform.

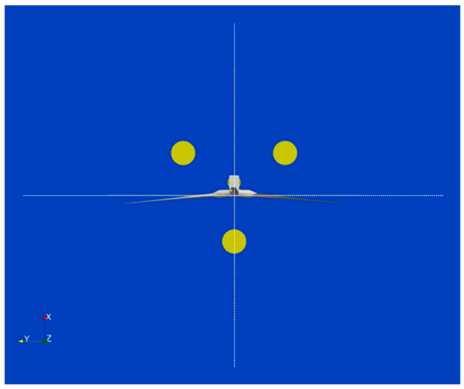

(**a**) Case 1, max. yaw: +0.06°

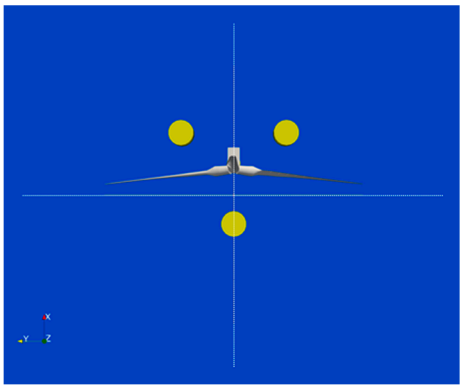

(**b**) Case 2, max. yaw: +0.05°

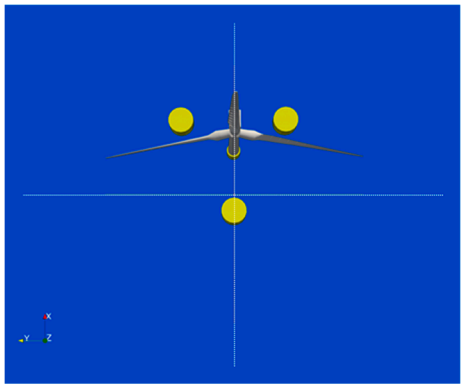

(**c**) Case 3, max. yaw: +0.29°

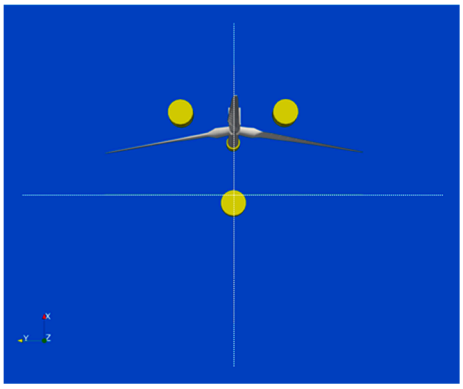

(**d**) Case 4, max. yaw: +0.25°

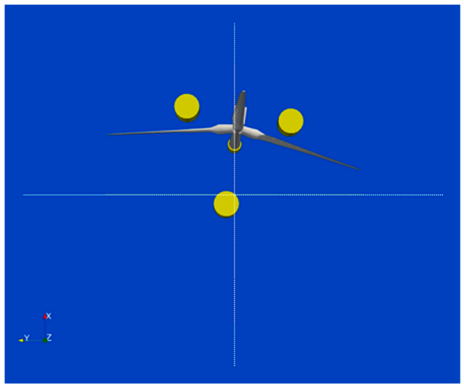

(**e**) Case 5, max. yaw: −7.74°

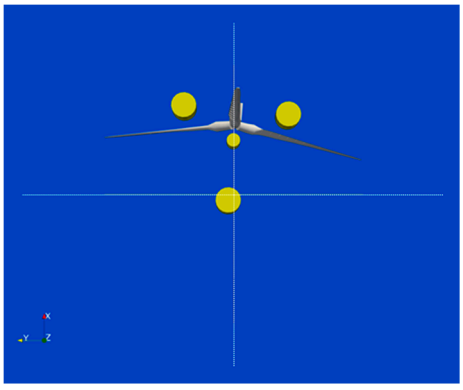

(**f**) Case 6, max. yaw: −4.74°

Figure 7. Snapshots when the maximum values of the platform's yaw motion occurred for the 6 cases.

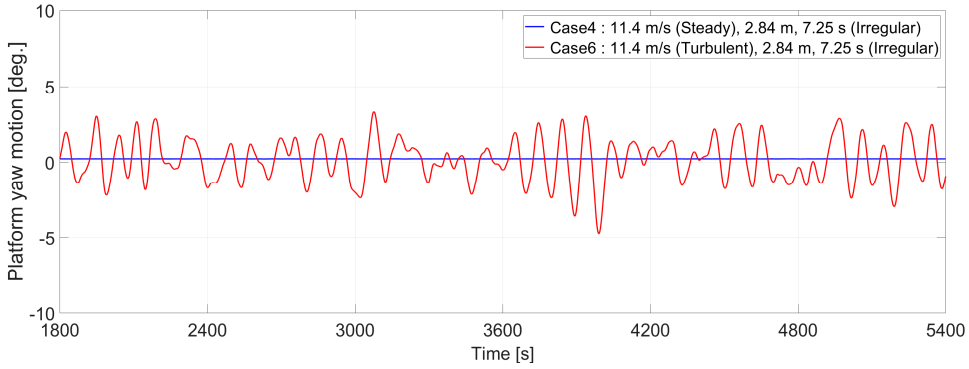

Figure 8. Time series of the platform's yaw motion for cases 4 and 6.

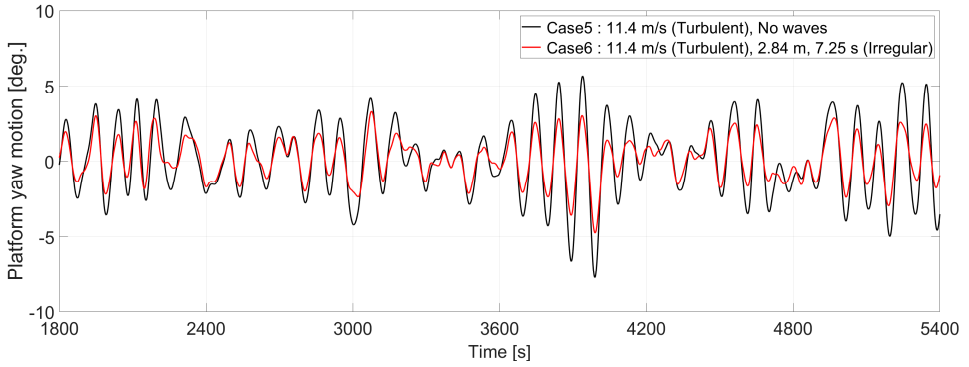

Figure 9. Time series of the platform's yaw motion for cases 5 and 6.

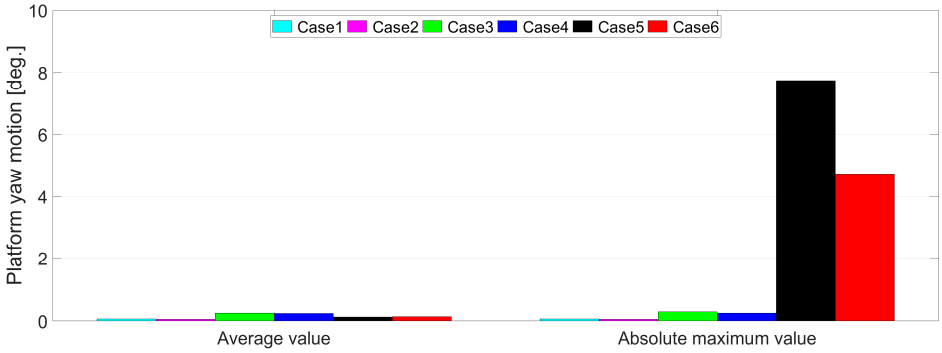

Figure 10. Average and absolute maximum values of the platform yaw's motion for all conditions.

3.2.2. Influence of the Platform Yaw's Motion

The wind turbine system controls the nacelle–yaw angle so that the rotating surface of the blades always faces the main direction of the wind in order to achieve maximum efficiency. Unlike the fixed wind turbine system, the control systems of the floating offshore wind turbine system need to consider not only the wind direction but also the platform's motion because the platform's motion occurs from the external force caused by the wind and waves. As can be seen from the previous results, it was confirmed that the platform's yaw motion occurred due to the gyroscope phenomenon and the aerodynamic instability in a large floating offshore wind turbine system, and how this platform's yaw motion affected loads and power was examined. Since the platform's yaw motion cannot be fixed in the analysis, the effect of the platform's yaw motion was replaced by adjusting the nacelle–yaw angle. The wind speed and rotor rotational speed used were rated, the wave condition was the same as mentioned in Section 2.2, and the output parameters were the platform's yaw motion, tower top's yaw moment, tower base's yaw moment and power.

Figure 11 shows the average of the absolute values of the output parameters according to nacelle–yaw angle. These results may appear linear because they show the average values over a sufficient time period except for the initial transients. In the results of the platform's yaw motion, it was confirmed that the platform's yaw motion was smaller when the nacelle–yaw angle was 1 to 6 degrees than when it was 0 degrees. In addition, it can be seen that the platform's yaw motion was relatively asymmetric compared to the other results based on a nacelle–yaw angle of 3 degrees, due to the influence of the gyroscope phenomenon. In the results of the tower top and tower base yaw moments, it was also confirmed that the nacelle–yaw angle at which the minimum tower top and tower base yaw moments appeared was 1 degree instead of 0 degree. It can be seen that the tower top and tower base yaw moments were generally symmetric based on a nacelle–yaw angle of 1 degree. In the results of the power, it was confirmed that the nacelle–yaw angle at which the maximum power appeared was 1 degree instead of 0 degree. Combining the above results, in a large floating offshore wind turbine system, a certain platform's yaw motion occurs even when the wind and waves act in the forward direction due to the gyroscope phenomenon and the aerodynamic instability due to the turbulent wind. In order to alleviate this phenomenon, some adjustment of the nacelle–yaw angle can be performed, which can maximize the power as well as minimize the platform's yaw motion, tower top and tower base yaw moments. Therefore, in this study, we confirmed we could find the optimal value of the nacelle–yaw angle by solving the multiobjective optimization problem.

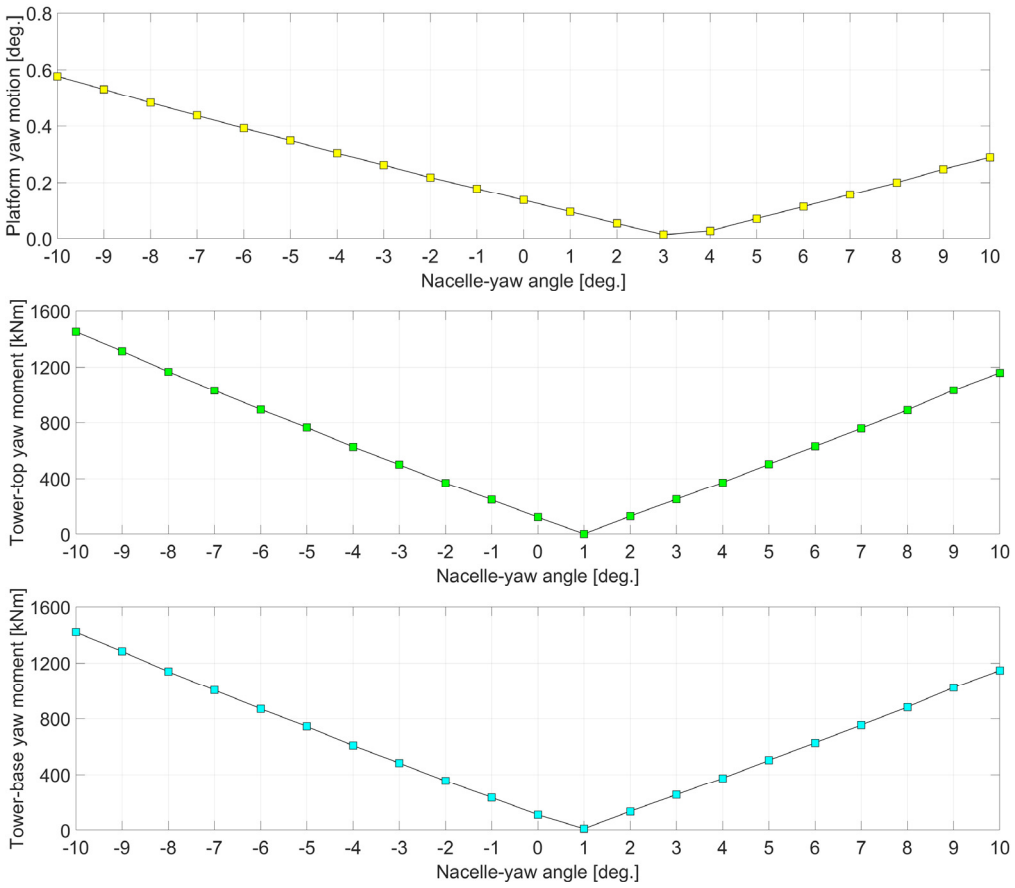

Figure 11. *Cont.*

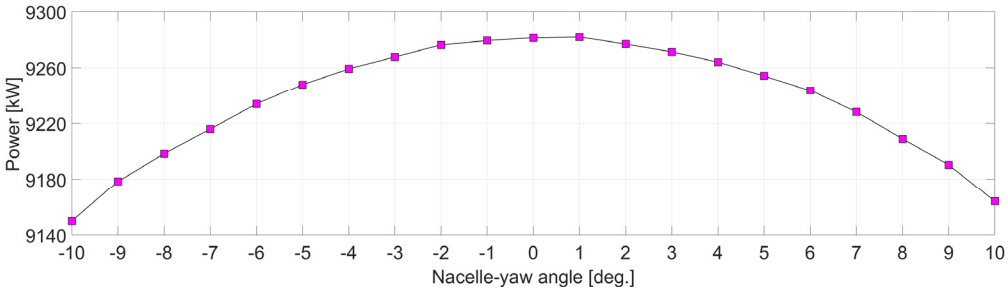

Figure 11. Average of the absolute values of output parameters according to nacelle–yaw angle.

Figure 12 shows the optimal curve of the nacelle–yaw angle by using the multiobjective optimization method, which is widely used in optimal problem fields. A multiobjective optimization method involves more than one objective function to be minimized or maximized. The goal of this study was to use this multiobjective optimization method to secure a structural stability by minimizing the tower top's yaw moment and to obtain good power generation performance by maximizing the power.

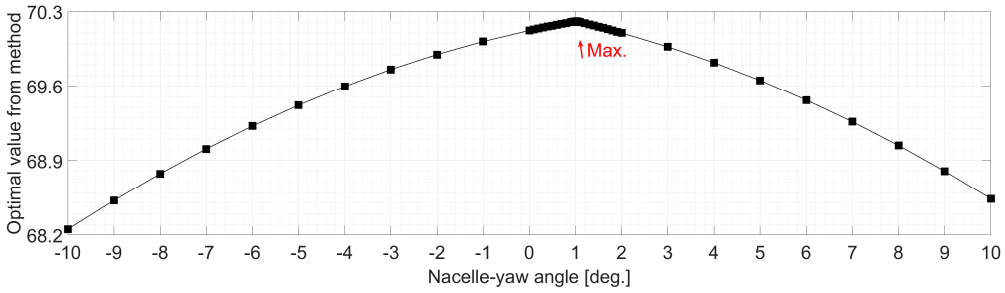

Figure 12. Optimal curve of the multiobjective optimization problem.

The multiobjective optimization function was made by finding quadratic and linear equations of the tower top's yaw moment and power, as shown in Figure 11. The multiobjective optimization function was written as follows:

$$f(x) = \left(ax^2 + bx + c\right) - (|\,px + q|\,) \tag{1}$$

where x is the nacelle–yaw angle, a means the coefficient of the quadratic term for the power in Figure 11, b means the coefficient of the linear term for the power in Figure 11 and c means the constant term for the power in Figure 11. Moreover, p means the coefficient of the linear term for the tower top's yaw moment in Figure 11 and q means the constant term for the tower top's yaw moment in Figure 11. In particular, the linear equation of the tower top's yaw moment was expressed as absolute values. As shown in Figure 12, it was confirmed that the maximum value of the multiobjective optimization function appeared when the nacelle–yaw angle was 1.02 degrees in this study. In summary, the large floating offshore wind turbine used in this study generated a constant platform's yaw motion, so if the nacelle–yaw angle was adjusted by about 1.02 degrees, the tower top's yaw moment could be minimized, and the power generated could be maximized. Figure 13 show the flowchart of the multiobjective optimization method used in this study.

3.3. Interval Angle of Incidence of Wind and Waves

In this study, the platform's motion, blade and tower's moments and fairlead and anchor tensions according to the interval angle of incidence of the wind and waves were confirmed. Table 5 shows the definition of the interval angle of incidence of the wind and waves used in this study, and the results were investigated with load diagrams and normalized values, respectively.

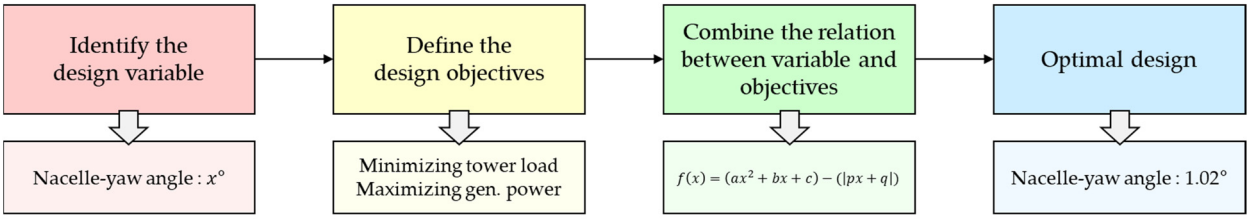

Figure 13. Flowchart of the multiobjective optimization method.

Table 5. Summary of the bins according to the interval angle of wind and waves.

Number of Bins	Interval Angle (°)	Angles between the Wind and Waves (°)
24	15	0, 15, 30, . . ., 315, 330, 345
12	30	0, 30, 60, 90, 120, 150, 180, 210, 240, 270, 300, 330
8	45	0, 45, 90, 135, 180, 225, 270, 315
6	60	0, 60, 120, 180, 240, 300

Figures 14–16 show the load diagrams of the output parameters according to the interval angles in order (top to bottom) except for the case where there is only one bin. These figures easily show whether or not the platform motion and loads with interval angles of incidence of the wind and waves are underestimated. In the results of the platform motion, the load diagrams gradually changed from the interval angles above 45 degrees, so an interval angle of at least 30 degrees should be used in the load analysis. In addition, the roll and pitch motions occurred asymmetrically even though the platform was symmetric on the left and right, which means that the influence of the large wind turbine rotating in one direction was greater than that of the wave directions. In the results of the blade and tower's moments, the load diagrams were very asymmetrical and spiky compared to the platform's motion. This means that the maximum value may not be predictable at an interval of 30 degrees. In the results of the fairlead and anchor motion, the load diagrams were quite well predicted with an interval angle of about 60 degrees.

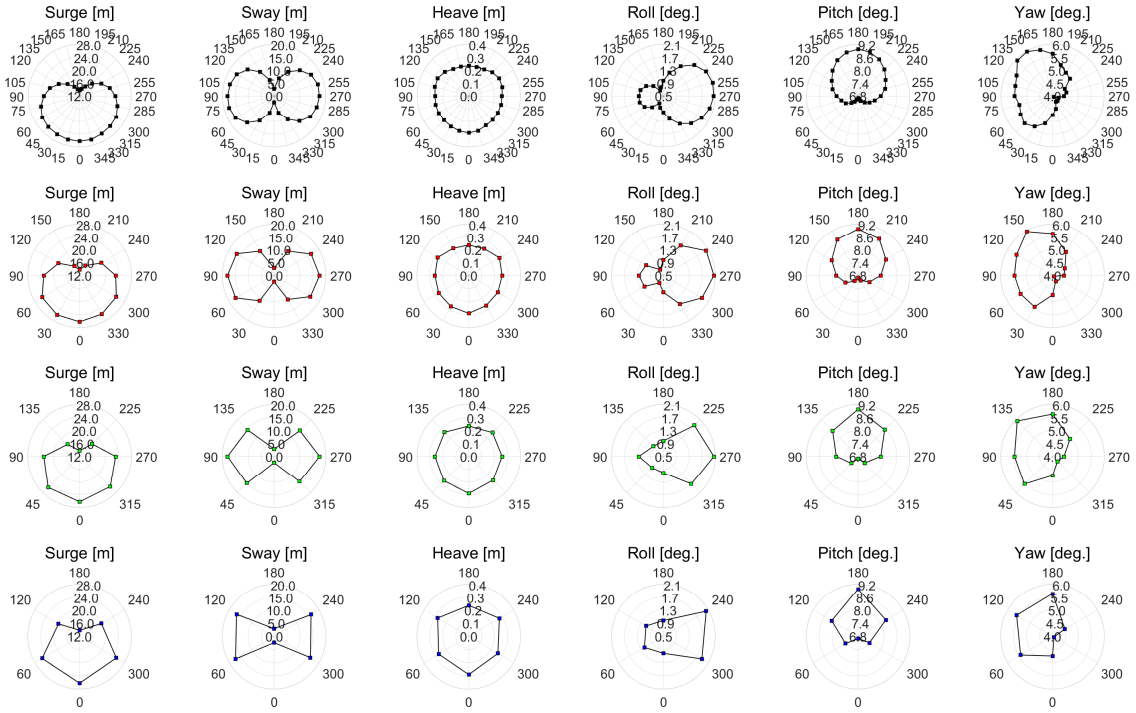

Figure 14. Maximum values of the platform's motion according to the interval angles.

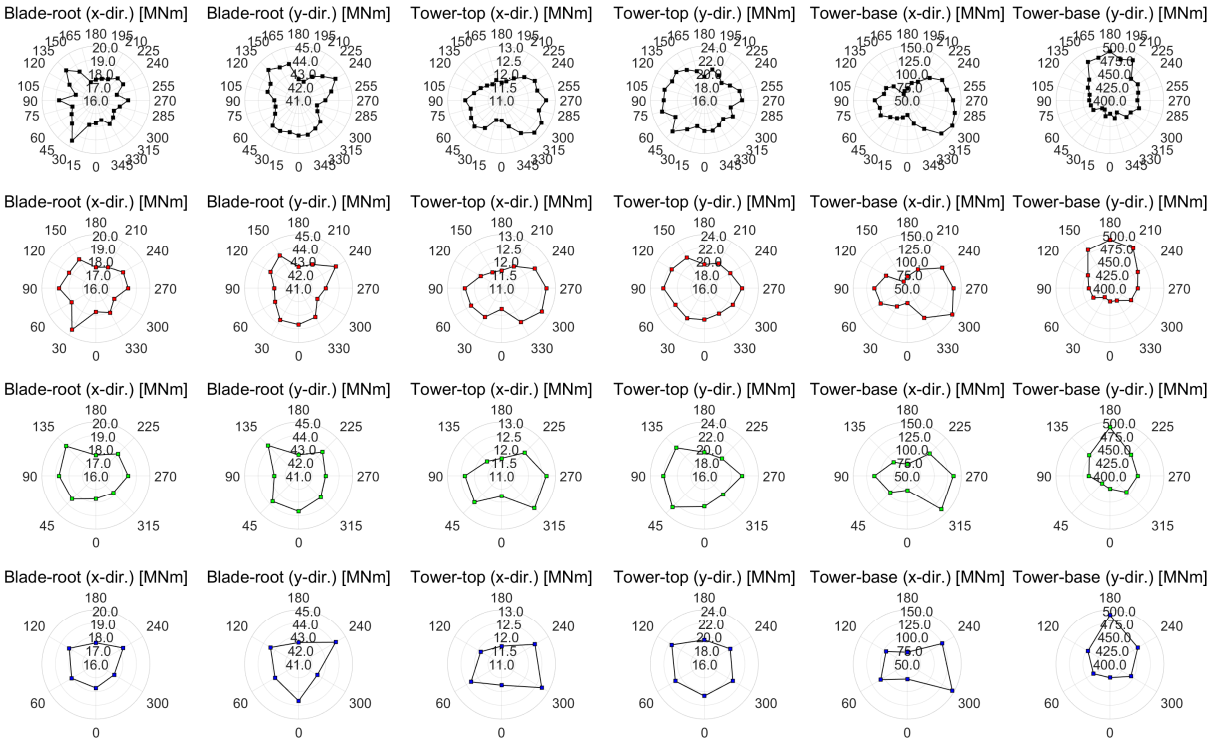

Figure 15. Maximum values of the blade and tower's moments according to the interval angles.

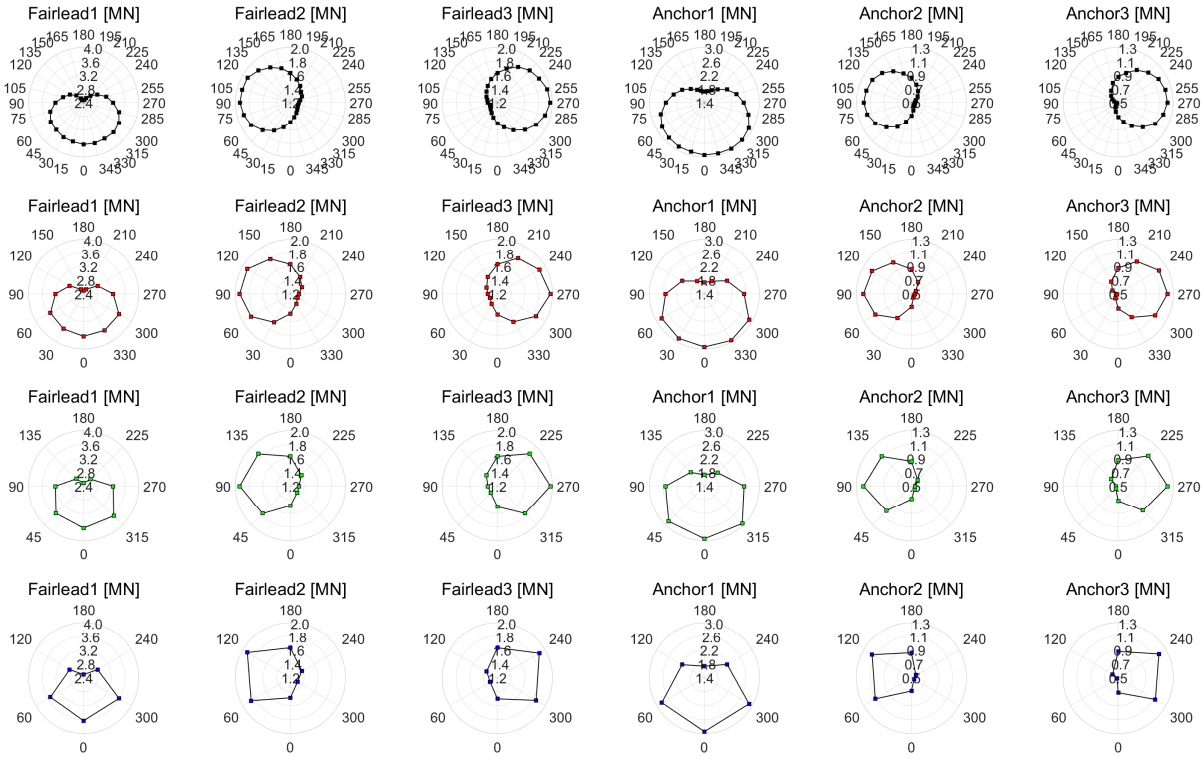

Figure 16. Maximum values of the fairlead and anchor tensions according to the interval angles.

Figure 17 shows the normalized values for the maximum platform's motion according to the interval angles. The maximum platform's motion can be predicted sufficiently even with the interval angle of incidence of the wind and waves proposed by Barj et al. and IEC61400-3-2. Figure 18 shows the normalized values for the maximum blade and tower's

moments according to the interval angles. In the tower top's moment (y-dir.) case, the maximum value could not be predicted at an interval of 30 degrees. This may result in a maximum value at small-interval angles. Figure 19 shows the normalized values for the maximum fairlead and anchor tensions according to the interval angles. The maximum fairlead and anchor tensions can be predicted sufficiently even with the interval angle of incidence of the wind and waves proposed by Barj et al. and IEC61400-3-2.

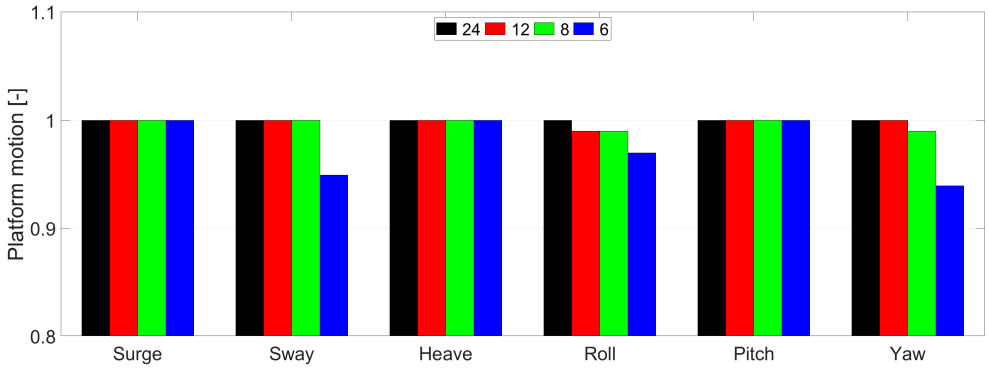

Figure 17. Normalized values for maximum platform's motion according to the interval angles.

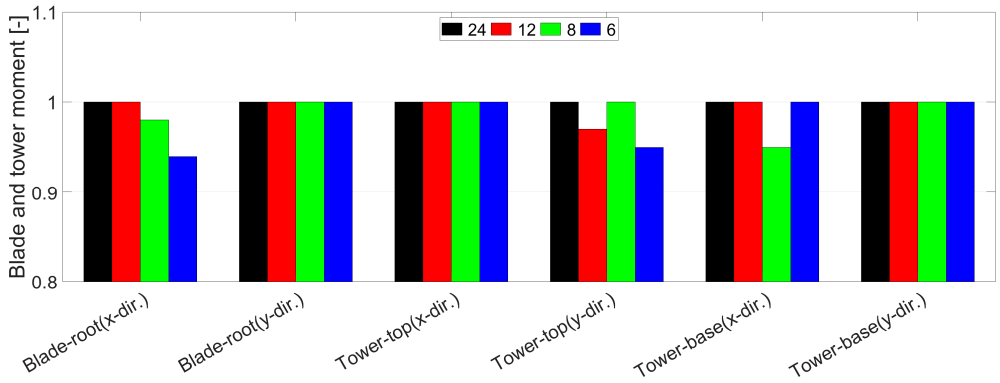

Figure 18. Normalized values for maximum blade and tower's moments according to the interval angles.

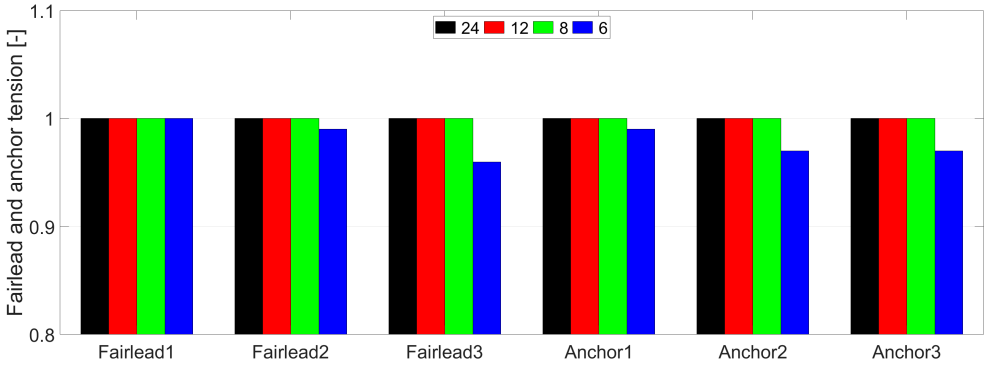

Figure 19. Normalized values for maximum fairlead and anchor tensions according to the interval angles.

4. Conclusions and Future Work

4.1. Conclusions

A numerical simulation was performed on the performance evaluation of the floating offshore wind turbine system according to the change in the direction of the incoming wind and waves. From a series of numerical simulation, the following conclusions are drawn:

- In the results of the platform's motion, the platform's motion occurred asymmetrically, and in particular, it could be seen that the platform's yaw motion occurred at more than 4 degrees even when the wind and waves acted in the forward direction due to the gyroscope phenomenon and the aerodynamic instability due to the turbulent wind. Since this can be larger in a larger turbine, it is necessary to confirm the load though a numerical simulation. In the results of the blade and tower's moments, is the results were very asymmetrical depending on the direction of the incoming wind and waves. Since the platform was submerged in water, but since the blade and tower directly faced the wind, it appeared more asymmetrical compared to the platform's motion.
- In a large floating offshore wind turbine system, a certain platform's yaw motion occurred even when the wind and waves acted in the forward direction due to the gyroscope phenomenon and the aerodynamic instability due to the turbulent wind. In order to alleviate this phenomenon, some adjustment of the nacelle–yaw angle could be made, which could maximize the power as well as minimize the platform's yaw motion, tower top's yaw moment and tower base's yaw moment. In this study, a multiobjective optimization function was used to find the optimal value of the nacelle–yaw angle, and it was found that the optimal value of the nacelle–yaw angle was 1.02 degrees.
- In the results of the interval angle of incidence of the wind and waves, even the 30-degree interval angle of incidence of the wind and waves suggested by Barj et al. and IEC61400-3-2 was sufficient to confirm the maximum value of each parameter. However, the load diagrams plots of the blade and tower's moments were very asymmetrical and spiky. This means that the maximum value may not be predictable at an interval of 30 degrees. In fact, the tower top's moment (y-dir.) in this study did not predict the maximum value at an interval of 30 degrees.

4.2. Future Work

Recently, the platforms have been enlarged and platforms having various shapes have been developed, and there are often cases where the wind turbine is installed on the side column rather than the center column of the platform. On the other hand, most of the existing studies and standards have only dealt with the NREL 5 MW reference wind turbine and simple cylindrical platforms (e.g., OC3 spar, OC4 Semi-submersible). Now, in order to improve the load predictability of a large floating offshore wind turbine system, it seems that the load analysis with a small interval angle of incidence of the wind and waves is needed. In future work, the platform's motion and loads will be evaluated by considering various shapes of platforms and the location where is wind turbine is installed. Combining these results, we will suggest a generalized interval angle of incidence of the wind and waves of a large floating offshore wind turbine system.

Author Contributions: Conceptualization, H.A. and Y.-J.H.; methodology, S.-g.C.; software, H.A.; validation, H.A.; formal analysis, S.-g.C. and C.-H.L.; investigation, Y.-J.H., S.-g.C. and C.-H.L.; resources, Y.-J.H.; data curation, H.A.; writing—original draft preparation, H.A.; writing—review and editing, K.-H.K.; visualization, H.A.; supervision, K.-H.K.; project administration, K.-H.K.; funding acquisition, K.-H.K. All authors have read and agreed to the published version of the manuscript.

Funding: This study was supported by a grant from the endowment project of "Development of core technology for integrated offshore green hydrogen production system" funded by the Korea Research Institute of Ships and Ocean Engineering (PES4361).

Institutional Review Board Statement: Not applicable.

Informed Consent Statement: Not applicable.

Data Availability Statement: Not applicable.

Acknowledgments: Not applicable.

Conflicts of Interest: The authors declare no conflict of interest.

References

1. Bachynski, E.E.; Kvittem, M.I.; Luan, C.; Moan, T. Wind-wave misalignment effects on floating wind turbines: Motions and tower load effects. *J. Offshore Mech. Arct. Eng.* **2014**, *136*, 4. [CrossRef]
2. Jonkman, J. *Definition of the Floating System for Phase IV of OC3*; National Renewable Energy Lab. (NREL): Golden, CO, USA, 2010.
3. Robertson, A.; Jonkman, J.; Masciola, M.; Song, H.; Goupee, A.; Coulling, A.; Luan, C. *Definition of the Semisubmersible Floating System for Phase II of OC4*; National Renewable Energy Lab. (NREL): Golden, CO, USA, 2014.
4. Barj, L.; Jonkman, J.M.; Robertson, A.; Stewart, G.M.; Lackner, M.A.; Haid, L.; Matha, D.; Stewart, S.W. Wind/wave misalignment in the loads analysis of a floating offshore wind turbine. In Proceedings of the 32nd ASME Wind Energy Symposium, Prince George's County, MD, USA, 13–17 January 2014.
5. Stewart, G.M. Design load analysis of two floating offshore wind turbine concepts. Ph.D. Thesis, University of Massachusetts, Amherst, MA, USA, 2016.
6. International Electrotechnical Commission. *Wind Energy Generation Systems-Part 3–2: Design Requirements for Floating Offshore Wind Turbines*; IEC TS: Geneva, Switzerland, 2019; pp. 61400–61403.
7. Oh, S.; Iwashita, T.; Suzuki, H. Numerical modelling and validation of a semisubmersible floating offshore wind turbine under wind and wave misalignment. *J. Phys. Conf. Ser.* **2018**, *1104*, 012010. [CrossRef]
8. Lyu, G.; Zhang, H.; Li, J. Effects of incident wind/wave directions on dynamic response of a SPAR-type floating offshore wind turbine system. *Acta Mech. Sin.* **2019**, *35*, 954–963. [CrossRef]
9. Jonkman, J.; Butterfield, S.; Musial, W.; Scott, G. *Definition of a 5-MW Reference Wind Turbine for Offshore System Development (No. NREL/TP-500-38060)*; National Renewable Energy Lab. (NREL): Golden, CO, USA, 2009.
10. Li, X.; Zhu, C.; Fan, Z.; Chen, X.; Tan, J. Effects of the yaw error and the wind-wave misalignment on the dynamic characteristics of the floating offshore wind turbine. *Ocean. Eng.* **2020**, *199*, 106960. [CrossRef]
11. Özinan, U.; Kretschmer, M.; Lemmer, F.; Cheng, P.W. Effects of yaw misalignment on platform motions and fairlead tensions of the OO-Star Wind Floater Semi 10MW floating wind turbine. *J. Phys. Conf. Ser.* **2020**, *1618*, 052081. [CrossRef]
12. Jonkman, J.M.; Buhl, M.L. FAST user's guide. *Gold. CO Natl. Renew. Energy Lab.* **2005**, *365*, 366.
13. Borg, M.; Mirzaei, M.; Brendmose, H. *D1. 2 Wind Turbine Models for the Design*; DTU, Public LIFES50 D; DTU: Roskilde, Denmark, 2015; p. 1.
14. Pegalajar-Jurado, A.; Bredmose, H.; Borg, M.; Straume, J.G.; Landbø, T.; Andersen, H.S.; Yu, W.; Müller, K.; Lemmer, F. State-of-the-art model for the LIFES50+ OO-Star Wind Floater Semi 10MW floating wind turbine. *J. Phys. Conf. Ser.* **2018**, *1104*, 012024. [CrossRef]
15. Yu, W.; Müller, K.; Lemmer, F.; Bredmose, H.; Borg, M.; Sanchez, G.; Landbo, T. *Public Definition of the Two LIFES50+ 10MW Floater Concepts*; LIFES50+ Deliverable: Stuttgart, Germany, 2017.
16. Jonkman, B.J. *TurbSim User's Guide*; National Renewable Energy Lab.(NREL): Golden, CO, USA, 2006.
17. Blusseau, P.; Patel, M.H. Gyroscopic effects on a large vertical axis wind turbine mounted on a floating structure. *Renew. Energy* **2012**, *46*, 31–42. [CrossRef]
18. Philippe, M.; Babarit, A.; Ferrant, P. Modes of response of an offshore wind turbine with directional wind and waves. *Renew. Energy* **2013**, *49*, 151–155. [CrossRef]